# Optimizing Energy Efficiency in Polling-Based Wireless Networks with Stability Constraints

Yi Xie and Rocky K. C. Chang
Department of Computing
The Hong Kong Polytechnic University
{csyxie,csrchang}@comp.polyu.edu.hk

***Abstract*— In this paper we consider the problem of minimizing the total energy for all devices in a wireless infrastructure network. The wireless devices use transmission power control and power saving mode to conserve energy. In particular we consider a polling-based MAC protocol which determines optimal power schedules (therefore the transmission rates) for all devices. Moreover, we have considered two grouping schedules: Phase Grouping (PG) and Mobile Grouping (MG). Through an iterative algorithm, we compute and compare the suboptimal energy consumptions for the two schedules based on the number of bits transmitted per joule of energy. Extensive results show that the MG schedule is much more energy efficient than the PG schedule, and the main sources of energy saving come from the reception and mode transition phases. Moreover, we evaluate the impact of an uncooperative user, who does not follow the optimal power allocation, on its own and others' energy-delay performance.**

## I. Introduction

Designing energy-efficient MAC protocols is an important issue to consider in wireless and mobile communications. In this paper we consider polling-based MAC protocols and particularly we consider two grouping schedules. In the *phase grouping* (PG) schedule, as illustrated in Figure 1, the uplink and downlink phases alternate between them. In the downlink phase, the AP broadcasts packets to all wireless devices, and each device is polled individually to send packets in the uplink phase. Therefore, using the power saving mode (PSM), a device can be put into sleep when it is not polled or receiving packets. On the other hand, the *mobile grouping* (MG) schedule groups the uplink and downlink phases for each wireless device. Each device stays in the sleeping state, except when it is polled by the AP for packet reception and transmission. Note that frequent transitions between the sleep mode and the active mode also consume a significant amount of energy.

Besides the PSM, we also employ transmission power control (TPC) [5] to reduce the energy consumption. The previous studies of many channel coding schemes have showed that the communication energy can be saved by transmitting packets with a lower transmission rate [8]. We adopt TPC with the convex rate-power curve derived from the Shannon's theorem. The optimal channel capacity is given by $C_{max} = W \times \log_2(1+\frac{S}{N})$ bps, where $W$ is the bandwidth in Hz, $N$ is the Gaussian noise power and $S$ is the signal power. Moreover, the actual transmission rate is given by $R = \alpha C_{max}$ bps, where $\alpha \in (0,1)$. By introducing an attenuation parameter $A$, the ratio of the transmission power $P$ to $S$, the power-rate relationship is

$$R = \alpha W \log_2(1 + P/(AN)). \quad (1)$$

Moreover, a commonly used metric for energy efficiency is the number of transmitted bits by consuming one joule of energy $z = \frac{R}{P}$. Note that $z$ can be increased by lowering $P$.

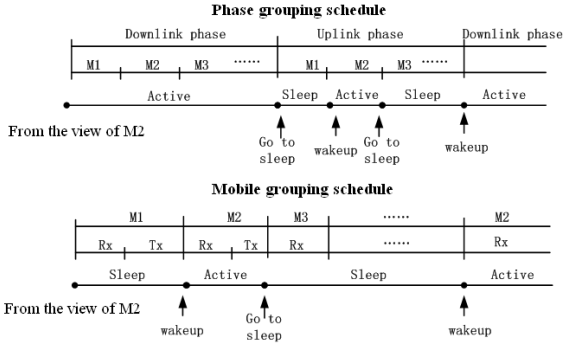


Fig. 1. Two grouping schedules for polling-based MAC protocols.

Most of the power-saving mechanisms will nevertheless degrade the communication and application performance. Therefore, many previous works considered optimal trade-offs between energy consumption and various performance metrics, such as throughput [9], delay [3], [4], [6], network utility [1], and error rate [5]. In our previous paper [7], we have solved the optimization problems which minimize the total energy consumption of *all* wireless devices in the network, subject to stability constraints. A device is stable if the packet delay (or queue length) is bounded in the sense of probability [2]. The objective of this paper is to further conduct a more holistic evaluation of the optimal schedules, including a delay-energy tradeoff and an energy efficiency evaluation based on $z$.

## II. System models

We use a cyclic-service queueing system to model the 2 grouping schedules. There are $c$ wireless devices in the network, which are serviced by an AP according to a fixed polling schedule. Each wireless device is modeled as a queue with infinite buffers, denoted by $q_i$ $(i = 1, \ldots, c)$, and the AP is modeled as a server. The server will leave the polling queue when it is empty or when all packets arrived before the server visits have been serviced. Packets are generated at

the queues for uplink transmissions to the AP, and packets are generated at the AP for downlink transmissions to the queues. The arrival processes of the uplink traffic and downlink traffic are assumed to be independent Poisson processes, with mean arrival rates equal to $\lambda_{u,i}$ and $\lambda_{d,i}$ for $q_i$, respectively. The uplink (downlink) service time processes, which are assumed to be independent and generally distributed, are denoted as $B_{u,i}(B_{d,i})$ for $q_i$, with mean equal to $b_{u,i}(b_{d,i}) < \infty$. Note that the mean service times are not constants due to the TPC.

In the model for the MG schedule, the server visits the queues in a deterministic and cyclic order: $q_1, q_2, \ldots, q_c, q_1, \ldots$. The downlink traffic has a higher priority over the uplink traffic in all queues. Moreover, there is a nonzero walk time involved in switching between queues, which models the wake-up period. The walk time process from $q_{i-1}$ to $q_i$, denoted by $SW_i$, is generally distributed with mean $s_i < \infty$, and $SW_i$ is independent of $SW_j, j \neq i$. We define the period, in which the server is serving $q_i$, as $q_i$'s *busy period*. The busy period is further divided into a uplink period $Tx_i$ and a downlink period $Rx_i$. On the other hand, the period, in which the server is away from $q_i$, is called the *vacation period* (from the $q_i$'s viewpoint). The cycle period $C_i$ is a sum of $q_i$'s busy period and the vacation period.

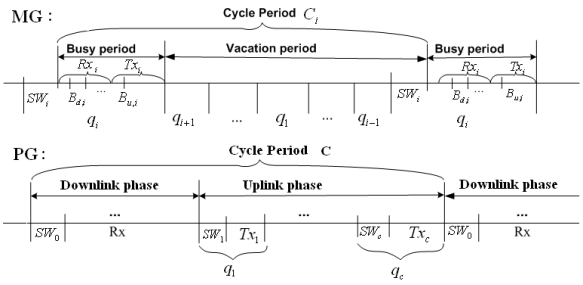


Fig. 2. System models of two grouping schedules

The model for the PG schedule is similar to the one for the MG schedule, except that we separate the downlink and uplink phases. In the uplink phase, the server again visits the queues in a fixed order, where uplink periods $Tx_i$ and $SW_i(\forall i)$ are defined similarly as before. The sum of $Tx_i$ and $SW_i$, $\forall i$ is regarded as the uplink phase. The downlink phase, on the other hand, is modeled as another queue with traffic generated by the AP. Unlike the MG schedule, the AP transmits all packets with the same transmission power and the same average transmission time $\overline{b_D}$. A walk time $SW_0$ is spent before all wireless devices are ready to receive data, which is generally distributed with mean $s_0$. The length of the downlink phase equals to the sum of the downlink period $R_x$ and $SW_0$. The cycle period $C$ is the sum of the uplink phase and the downlink phase.

## III. Network-centric energy optimization

Let $E_i$ be the energy consumed by $q_i$ during a cycle. We are interested in computing the average of $E = \sum_{j=1}^{c} E_j$ for the MG and PG schedules. According to the Law of Large Numbers, the statistical average converges to its expectation, $\mathbf{E}[E]$. As for the power constraints, the power of the wireless devices is assumed to operate within $[P_{min}, P_{max}]$. On the other hand, let the AP's transmission power when sending data to $q_i$ be $P_{AP,i}$ ($\leq P_{MAX}$). The second set of constraints are on the device (queue) stability. From the analysis results of [2], the total workload $\rho = \sum_{i\forall} \lambda_i b_i$ must be less than 1, if the whole network is stable. In order to match the standard formulation of the optimization problem, the stability constraint is relaxed to $\rho \leq 1$.

In order to optimize the MG schedule, we allocate transmission power vectors $\mathbf{P^*}_{AP}$ in the AP and $\mathbf{P}^*$ in wireless devices, which are determined by two optimal service time vectors $\mathbf{b}_d^*$ and $\mathbf{b}_u^*$, respectively. According to (1) and $SNR_i(\mathbf{P}) = \frac{P_i/g_{ii}}{N_i + \sum_{j\neq i}^{c} P_j g_{ij}}$ defined in [1], the transmission time per packet is $B_i = \frac{F_i}{WR_i} = \frac{2F_i/\alpha W}{\log_2(1+SNR_i(\mathbf{P}))}$, where $F_i$ be the r.v. for $q_i$'s packet size in bits. Besides, $a_{ij}$ $(i, j = 1, \ldots, c)$ denotes the attenuations/gains between the wireless channels. $N_i$ is the noise power of the wireless channel for $q_i$. Assuming that the transmission powers in both directions are the same as $P_i$, $a_{ij} = 0$, $\forall i \neq j$ and $SNR \gg 1$, we have $P_i(b_i) \approx K_i \times 2^{H_i/b_i}$, where $K_i = a_{ii}N_i$ and $H_i = 2\mathbf{E}[F_i]/\alpha W$.

Besides, assume that all queues have the same power consumptions in the receiving, transiting and sleeping modes, denoted by $P_R$, $P_I$ and $P_V$, respectively. The transmission power of the wireless devices and AP is always less than $P_{max}$ but larger than $P_{min}$. Denote the ratio of the downlink traffic as $\beta_i = \frac{\lambda_{d,i}}{\lambda_{d,i}+\lambda_{u,i}}$. The optimization problem of the MG schedule is given by (2) when assuming $\mathbf{P}_{AP} = \mathbf{P}$.

$$\begin{aligned} \min_{\mathbf{b}} \quad & \frac{s\sum_{j=1}^{c} \rho_j[(1-\beta_j)P_j + \beta_j P_R]}{1-\rho} + s(P_I + P_V\frac{c-1}{1-\rho}) \\ s.t. \quad & \sum_{j=1}^{c} \lambda_j b_j - 1 \leq 0. \\ & H_i/[\log_2(P_{max}/K_i)] - b_i \leq 0, \ \forall i. \\ & b_i - H_i/[\log_2(P_{min}/K_i)] \leq 0, \ \forall i. \end{aligned} \tag{2}$$

Similarly, we can obtain the optimization problem for the PG schedule, where $\mathbf{P}_{AP}$ operates on $P_{max}$.

$$\begin{aligned} \min_{\mathbf{b_d},\mathbf{b_u}} \quad & (P_I - P_V)(cs_0 + s) + \frac{s_0 + s}{1-\rho'}[\sum_{j=1}^{c} P_j\rho_{u,j} + \\ & c(P_R - P_V)\rho_D + P_V\sum_{j=1}^{c}(1-\rho_{u,j})] \\ s.t. \quad & \sum_{j=1}^{c} \lambda_{d,j}\overline{b_D} + \sum_{j=1}^{c} \lambda_{u,j} b_{u,j} - 1 \leq 0. \\ & H_i/[\log_2(P_{max}/K_i)] - b_{u,i} \leq 0, \ \forall i. \\ & b_{u,i} - H_i/[\log_2(P_{min}/K_i)] \leq 0, \ \forall i. \\ & H_i/[\log_2 P_{MAX}/K_i] - b_{d,i} \leq 0, \ \forall i. \end{aligned} \tag{3}$$

According to the Karush-Kuhn-Tucker (KKT) conditions, we obtain two propositions which provide the necessary conditions for optimal solutions.

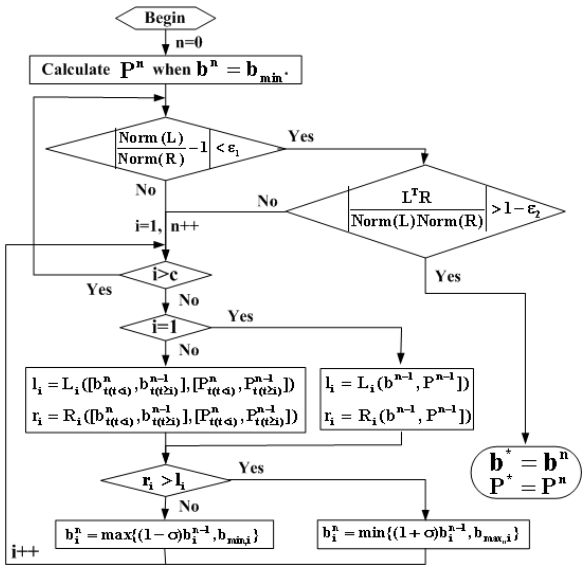


Fig. 3. An iterative algorithm for the MG schedule.

*Prop. 1:* In the MG schedule, if all wireless devices do not transmit data using their extreme power, $\mathbf{b}^*$ must satisfy $\mathbf{L}(\mathbf{b}^*) = \mathbf{R}(\mathbf{b}^*)$, where $L_i(\mathbf{b}) = [(1-\beta_i)P_i(b_i) + \beta_i P_R](1-\rho) + P_V(c-1) + \sum_{j=1}^{c} \rho_j[(1-\beta_j)P_j(b_j) + \beta_j P_R]$ and $R_i(\mathbf{b}) = (1-\beta_i)P_i(b_i)(1-\rho)\ln(\frac{P_i(b_i)}{K_i})$.

*Prop. 2:* In the PG schedule, if all wireless devices do not transmit data using their extreme power, $\mathbf{b}^*_{\mathbf{u}}$ must satisfy $\mathbf{L}(\mathbf{b}^*_{\mathbf{u}}) = \mathbf{R}(\mathbf{b}^*_{\mathbf{u}})$, where $L_i(\mathbf{b}_u) = P_i(b_{u,i})(1-\rho) + \sum_{j=1}^{c} \rho_j P_j(b_{u,j}) + P_V(c-1+\rho_D)$ and $R_i(\mathbf{b}_u) = P_i(b_{u,i})(1-\rho)\ln\frac{P_i(b_{u,i})}{K_i}$.

### A. An iterative algorithm

Based on Props. 1 and 2, we have devised iterative algorithms to solve (2) and (3), respectively. Here we just discuss the algorithm for the MG schedule, which is given in Figure 3. The algorithm essentially attempts to approach $\mathbf{L}(\mathbf{b}^*) = \mathbf{R}(\mathbf{b}^*)$ as close as possible. Therefore, the algorithm terminates when these two vectors are close enough, such that $|\frac{Norm(\mathbf{L})}{Norm(\mathbf{R})} - 1| < \varepsilon_1$ and $|\frac{\mathbf{L}^T\mathbf{R}}{Norm(\mathbf{L})Norm(\mathbf{R})}| > 1-\varepsilon_2$, where $\varepsilon_1$ and $\varepsilon_2$ are accuracy tolerance parameters. Inside the iterative loop, $R_i$ decreases monotonically with $b_i$. Therefore, in the $m$th iteration for $q_i$, if $R_i > L_i$, we increase $b_i^{m-1}$ by a step size of $\sigma \in (0,1)$; otherwise, we decrease $b_i^m$ by $\sigma$.

The stability constraints and power constraints jointly determine the feasible region for the transmission rates. Given $[P_{min}, P_{max}]$, when $\boldsymbol{\lambda}$ increases, $b_{min,i}$ is more likely to be determined by $P_{max}$, but $b_{max,i}$ is more likely to be determined by the stability constraint. For example, consider a tagged queue $q_T$ and other queues are identical. The arrival rate of $q_T$ is increased while that of other queues are kept at 50p/s. As shown in Figure 4, when $\lambda_{q_T}$ increases, the minimal service time of $q_T$ ($b_{min,t}$) and that of other queues ($b_{min,o}$) converge to $b^P_{min}$ which is determined by $P_{max}$. On the contrary, when $\lambda_{q_T}$ decreases, the maximal service times of $q_T$ ($b_{max,t}$) and that of other queues ($b_{max,o}$) converge to $b^P_{max}$ which is determined by the $P_{min}$. Moreover, given $\boldsymbol{\lambda}$, a reduction in $P_{min}$ ($P_{max}$) would increase $b^P_{max,i}$ ($b^P_{min,i}$), but decrease $b^\rho_{min,i}$ ($b^\rho_{max,i}$).

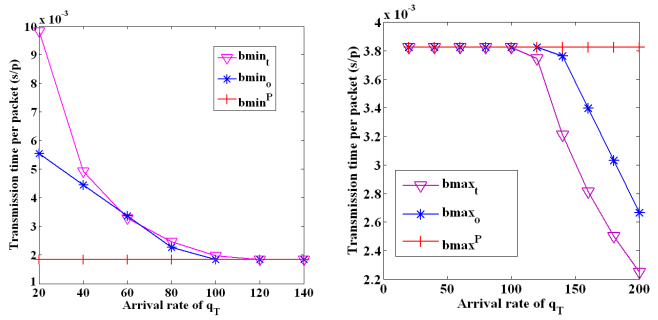


(a) $b_{min}$ in the feasible region (b) $b_{max}$ in the feasible region

Fig. 4. The impacts of stability and power constraints on the feasible region.

The iterative algorithm yields a global optimal solution when $c = 2$; however, it is not the case for $c > 2$. Our extensive experiment results show that the algorithm converges quite quickly, i.e. $n \leq 50$ in most cases. Moreover, it works particularly well when the traffic arrival intensity is small, i.e., $\boldsymbol{\lambda}^T \mathbf{b}_{min} < 0.5$. We have also applied the Gauss-Siedel iteration to reduce the convergence time.

## IV. Performance Evaluation

The experiment results presented in this section are based on the following settings: $W = 1MHz$, $P_R = 2W$, $P_I = 1W$, and $P_V = 0.05W$. The power constraints are $P_{MAX} = P_{max} = 10W$ and $P_{min} = 1W$.

### A. Comparing the energy efficiency for the MG and PG schedules

In this section we compare the energy efficiency of the two grouping schedules based on the metric $z$. A possible comparison method is to obtain and compare their optimal power allocations under the same setting. Unfortunately, optimizing the grouping schedules directly based on $z$ is extremely difficult. Therefore, we instead obtain optimal schedules based on the average energy consumed in a cycle, i.e., solutions to (2) and (3). We then compare these optimal schedules based on $z$, and the values of $z$ for the optimal schedules are denoted as $z_{MG}$ and $z_{PG}$ for the MG and PG schedules, respectively. As we will show, the MG optimal schedule outperforms the PG optimal schedule, i.e., $z_{MG} > z_{PG}$. The comparison results to follow are based on symmetric systems in which the arrival rate $l$, the channel condition, and the packet size distributions are the same for all queues.

Figure 5 presents the comparison results for the case of $k = 0.5$, which represents a 50-50 mix of the uplink and downlink traffic. The figure shows that the optimal MG schedule is

more energy efficient than the optimal PG schedule, because $z_{MG}/z_{PG} > 1$ for all cases. Moreover, $z_{MG}/z_{PG}$ increases with $c$ and $l$. That is, the energy efficiency gap between the two schedules increases with $l$ and $c$. Furthermore, we repeat the experiments with different downlink-uplink traffic mix, and the results are shown in Table I. The comparison results remain the same for these cases. Besides, the gap becomes more prevalent when there is a higher proportion of downlink traffic. Furthermore, $z_{MG}/z_{PG}$ increases with $c$ for a given $k$, and $z_{MG}/z_{PG}$ increases with $k$ for a given $c$.

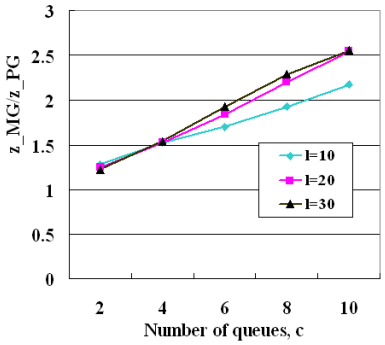


Fig. 5. An energy efficiency comparison with $\boldsymbol{\lambda}$=$l * e_c$ and $\boldsymbol{\beta}$=$0.5 * e_c$.

TABLE I

$z_{MG}/z_{PG}$ WITH $\boldsymbol{\beta}$=$k * e_c$ AND $\boldsymbol{\lambda}$=$20 * e_c$.

| c | 2 | 4 | 6 | 8 | 10 |
|---|---|---|---|---|---|
| $k$=0.2 | 1.26 | 1.42 | 1.53 | 1.67 | 1.80 |
| $k$=0.5 | 1.25 | 1.52 | 1.84 | 2.20 | 2.55 |
| $k$=0.8 | 1.28 | 1.76 | 2.22 | 2.80 | 3.44 |

To probe further, we identify the factors that are responsible for the MG schedule's higher energy efficiency. To this end, we decompose the total energy consumption into 4 components—energy due to receptions (Rx), transmissions (Tx), mode transitions (SW), and sleeping (V). We plot the results for both schedules in Figure 6(a) for $c = 3$. The figure clearly indicates that the MG schedule is able to save a significant amount of energy during the reception and mode transition phases. Since the PG schedule broadcasts in the downlink channel, all wireless devices have to be in the active mode, thus consuming much more energy. Moreover, each device in the PG schedule performs more mode transitions. As for the energy consumed during the transmission and sleeping mode, the MG and PG schedules consume almost the same amount of energy.

If we change the distribution of the traffic arrival rates while keeping the total traffic rate unchanged, it is interesting to observe that the energy consumptions of the 4 components will not change. For example, the experiments with $\boldsymbol{\lambda} = [30; 60; 90]$ and $\boldsymbol{\lambda} = [10; 50; 110]$ have the same results as that in Figure 6(a). In other words, the total arrival rate determines the energy consumption under the optimal schedules, instead of the individual ones, when other parameters and conditions are unchanged.

Using the cycle time, we can write the energy efficiency metric as $z = (\sum_{i=1}^{c} \lambda_i \mathbf{E}[C^*])/\mathbf{E}[E^*]$. Therefore, given $\boldsymbol{\lambda}$, $z_{MG} > z_{PG}$ implies that $\mathbf{E}[C^*_{MG}]/\mathbf{E}[C^*_{PG}] > \mathbf{E}[E^*_{MG}]/\mathbf{E}[E^*_{PG}]$. All of our experiments support that $\mathbf{E}[C^*_{MG}]/\mathbf{E}[C^*_{PG}] > \mathbf{E}[E^*_{MG}]/\mathbf{E}[E^*_{PG}]$, e.g. the results given in Figure 6(b). Besides, $\mathbf{E}[C^*_{MG}]/\mathbf{E}[C^*_{PG}]$ increases faster than $\mathbf{E}[E^*_{MG}]/\mathbf{E}[E^*_{PG}]$ as $c$ increases. This can explain why $z_{MG}/z_{PG}$ increases with $c$ which were discussed earlier.

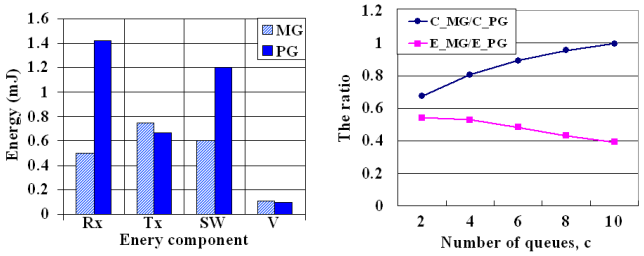


(a) Comparisons based on the 4 components with $\boldsymbol{\lambda}$ =[60;60;60]and $k = 0.5$.

(b) Comparison of the energy consumptions per cycle and the cycle time with $\boldsymbol{\lambda}$=$20 * e_c$ and $k = 0.5$.

Fig. 6. Comparing the energy efficiency for the MG and PG optimal schedules.

### B. Effect of an uncooperative user

So far we have assumed that all users adopt the optimal power allocations computed by the iterative algorithms. In this section we relax this assumption and study the effect of an uncooperative user on himself and others. Since the space is limited, we only discuss the MG schedule for a symmetric system with $\boldsymbol{\lambda} = 60e_4$ and $\boldsymbol{\beta} = 0.5e_4$. In order to have a more comprehensive evaluation, we include the delay performance as well which is obtained from simulations. The iteration algorithm, on the other hand, gives the optimal power allocation $\mathbf{P}^* = P^*e_4$, and the delay performance for the optimal schedules are indicated by superscript $*$. Moreover, we consider a tagged queue $q_T$ as the only uncooperative user, and his transmission power is $gP^*$, where $g$ is a change parameter. In the following, we label the results for $q_T$ with subscript $t$, the results of other queues using $P^*$ with subscript $o$, and the results of the whole system with subscript $s$.

We first evaluate how the uncooperative user affects the energy efficiency performance. Denote the total energy consumption per cycle by $\xi$ and that with the optimal power allocation $\mathbf{P}^*$ as $\xi^*$. Since $\xi^*$ is the minimum value, we define the *energy reduction ratio* (ERR) of the whole system under a nonoptimal schedule ($g \neq 1$) as $(\xi^* - \xi_s)/\xi^*$, which is always negative. Figure 7 shows the values of the ERR when $q_T$ uses a higher (lower) power than the optimal one, i.e., $g > 1$ ($g < 1$). The case of $g = 1$ corresponds to the optimal power; therefore, the ERR for $g = 1$ is 0. When $q_T$ uses a higher power, it will consume more energy while other queues may receive a little benefit on energy saving. As the figure shows, the total energy consumption still increases. On the other hand, if $q_T$ uses a

lower power, its energy consumption per cycle can be reduced; but in most cases the total energy consumption is still higher.

We now evaluate how the uncooperative user affects the average delay of the downlink and uplink traffic, which is denoted as $d$. The *delay reduction ratio* (DRR) is similarly defined as $(d^* - d)/d^*$ and $d^*$ is the delay for an optimal MG schedule. As shown in Figure 7, when $q_T$ uses a higher power ($g > 1$), the average delay of the downlink and uplink traffic in each queue decreases; therefore, the average delay for the whole system also decreases. On the other hand, when $q_T$ uses a lower power ($g < 1$), the delay performance will degrade in each queue as well as the entire system. Moreover, it is possible to improve the delay performance at the cost of a higher energy consumption. That is, there is a tradeoff between the energy conservation and the delay reduction, to be discussed next.

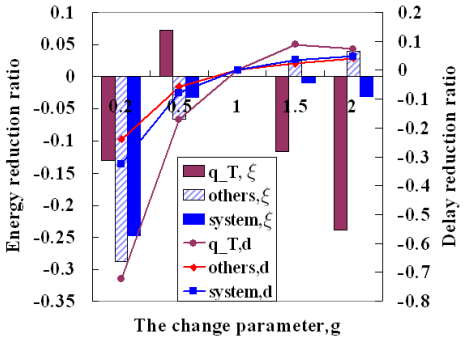


Fig. 7. Energy reduction ratio and delay reduction ratio in the presence of an uncooperative user.

Lastly we evaluate effect of the uncooperative user on both the delay and energy. To this end, we introduce a *delay-energy tradeoff metric* $\varphi = (1-m)\frac{d^*-d}{d^*} + m\frac{\xi^*-\xi}{\xi^*}$, where $m$ is a tradeoff parameter. The higher $\varphi$ is, the better delay-energy tradeoff is. Note that the special cases of $m = 1$ and $m = 0$ correspond to the ERR and DRR, respectively. Using $m = 0.5$, we compute the trade-off metric and the results are given in Figure 8(a). The figure shows that $q_T$ cannot improve its delay-energy tradeoff as long as it changes its optimal transmission power, i.e. $\varphi_t < 0$ when $g \neq 1$. However, other queues will benefit a little when $q_T$ uses a higher transmission power, because $\varphi_o > 0$ when $g > 1$. For the whole system, our optimal solution achieves the highest $\varphi_s$ when $m > 0.5$, as shown in Figure 8(b). Even when the delay-energy tradeoff metric is dominated by the delay performance, i.e., $m < 0.5$, the nonoptimal solutions achieve only a little higher $\varphi_s$ than that of the optimal solution. These analytical results can be obtained and analyzed similarly for $c \neq 4$ and asymmetric systems.

## V. Conclusions

We have considered the problem of optimizing energy efficiency for polling-based MAC protocols using the transmission power control and power saving mode. The objective is to minimize the total energy consumption for all wireless devices

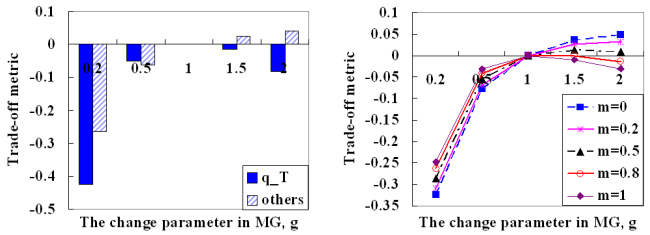


(a) Delay-energy tradeoff of queues ($\varphi_t$ and $\varphi_o$), $m = 0.5$

(b) Impact of $m$ on $\varphi_s$ in the system

Fig. 8. Delay-energy tradeoff metric in the presence of an uncooperative user.

under stability constraints imposed by the network capacity and power limitations. Moreover, we consider two grouping schedules: mobile grouping (MG) and phase grouping (PG). Based on optimization formulations, we have devised iterative algorithms to come up the optimal power allocations for both schedules. One of the main results is that the MG schedule is much more energy efficient than the PG schedule based on the number transmitted bits per joule of energy. By grouping the uplink and downlink transmission for each wireless device, the MG schedule can significantly reduce the amount of energy consumed during the reception and mode transition phases. Another important result is that an uncooperative user could not benefit from the delay and energy performance. That is, there are incentives for users to adopt the optimal power allocations computed by the iterative algorithm.

## Acknowledgment

The work described in this paper was partially supported by a grant from the Research Grant Council of the Hong Kong Special Administrative Region, China (Project No. PolyU 5146/01E). We also thank the reviewers for their helpful comments.

## References

[1] M. Chiang and J. Bell. Balancing supply and demand of bandwidth in wireless cellular networks: Utility maximization over powers and rates. In *Proc. IEEE INFOCOM*, 2004.

[2] M. Ferguson and Y. Aminetzah. Exact results for nonsymmetric token ring systems. *IEEE Trans. Commun.*, 33(3), 1985.

[3] T. Holliday, A. Goldsmith and P. Glynn. Optimal power control and source-channel coding for delay constrained traffic over wireless channels. In *Proc. IEEE ICC 2002*.

[4] C. Schurgers, V. Raghunathan and M. Srivastava. Modulation scaling for real-time energy aware packet scheduling. In *Proc. IEEE GLOBECOM*.

[5] D. Qiao, S. Choi, A. Soomro and K. Shin. Energy-efficient PCF operation of IEEE 802.11a wireless LAN. In *Proc. IEEE INFOCOM*, 2002.

[6] P. Nuggehalli, V. Srinivasan and R. Rao. Delay constrained energy efficient transmission strategies for wireless devices. In *Proc. IEEE INFOCOM*, 2002.

[7] Y. Xie and K. C. Chang. Stability-constrained optimization for energy efficiency in polling-based wireless networks. In *Proc. VALUETOOLS*, 2006.

[8] A. Tarello, J. Sun, M. Zafer and E. Modiano. Minimum energy transmission scheduling subject to deadline constraints. In *Proc. WIOPT*.

[9] F. Zhang and S. Chanson. Throughput and value maximization in wireless packet scheduling under energy and time constraints. In *Proc. 24th IEEE RTSS*, 2003.